Impact Localization in Inkjet-Printed Tactile Grid Sensor with Echo State Network

Shahrin Akter and Mohammad Rafiqul Haider
Department of Electrical Engineering and Computer Science
University of Missouri-Columbia
Columbia, MO, USA
{shahrin.akter, mhaider}@missouri.edu

***Abstract*—Tactile sensors with impact localization are becoming an essential part in automotive, aerospace, and civil engineering for damage assessment, safety assurance and structural monitoring. Inkjet printing is on rise for its eco-friendliness, cost-efficiency, low power consumption and quick design iteration ability. However, its minimal fabrication process results in operational challenges. These challenges can be mitigated by integrating artificial intelligence with inkjet printed sensors to enhance their performance. Among all artificial intelligences, echo state networks are gaining recognition for their low computational demands and hardware compatibility. This study developed an inkjet-printed tactile grid sensor with an echo state network for impact localization. The sensitivity of sensor was assessed through a pencil drop experiment, with data transformation across time and magnitude domains to improve network adaptability. Hyperparameters of the model were fine-tuned through sequential search. Developed echo state network with grid tactile sensor demonstrated high accuracy, pinpointing the impact location of pencil drops with an impressive precision rate of 94.89%.**

***Index Terms*—Echo state network, Inkjet printing technology, Reservoir computing, Tactile grid sensor, .**

I. Introduction

The rise of the Internet of Things (IoT) has significantly boosted the need for monitoring sensors in sectors like healthcare [1] [2], industrial automation [3], and robotics. In the automotive and aerospace industry, continuous monitoring and precise impact detection through tactile sensors are crucial for maintaining vehicle safety and structural integrity, as well as for pinpointing and evaluating the extent of any damage [4] [5]. In the realm of civil engineering, these sensors are indispensable for detecting potential structural damage, thereby aiding in the upkeep of infrastructure [6]. Additionally, the synergy of artificial intelligence with sensor technology is pushing the boundaries of real-time monitoring, classification, and predictive analysis. Employing inkjet printing to embed these sophisticated technologies onto flexible substrates brings several advantages, including reduced size, lower costs, and better environmental sustainability which is paving the way for mass production of sensor networks.

In the realm of technology, there's a pronounced shift towards making devices smaller. This miniaturization trend is driven by the consumer demand for more portable, space-efficient, and integrated technologies. Smaller devices often need to be cost-effective, especially when intended for mass production. Alongside this rising demand for miniaturization, there is an expectation for sensors to deliver enhanced accuracy in large-scale production. Inkjet printing technology emerges as a key player, meeting these needs low cost, energy efficient and compact while also offering the added advantage of being eco-friendly [7] [8]. Moreover, inkjet printed technology can be implemented in a wide range of flexible substrates. Nonetheless, inkjet printing may not always achieve the same precision as conventional silicon-based approaches due to its simplified and sophisticated fabrication process. This gap can be bridged by integrating artificial intelligence with inkjet printing, a combination that promises to amplify sensor capabilities and precision [9]. The combination of artificial intelligence and inkjet printing technology offers the potential to develop a sensor ecosystem that is not only cost-effective and energy-efficient but also exhibits improved performance.

Over the past few decades, in the realm of artificial intelligence, Reservoir Computing (RC) has demonstrated superior performance compared to other machine learning models in analyzing time series data for IoT devices. RC is a framework for computation used particularly in recurrent neural network settings. It is distinguished by its unique approach to handling the internal state. Among different RC methods, Echo State Network (ESN) has emerged as a prominent alternative to gradient descent-based neural networks due to its better convergence and simpler computational requirements, which makes it more practical and suitable for hardware implementation. Previously, through inkjet printing, neurons for a RC [10] are designed, as well as vibration and proximity sensor [11], tactile sensor [12] is designed. In our work, we have designed a efficient inkjet printed grid tactile sensor for impact localization and the sensor is combined with an ESN network to make the sensor more efficient than conventional inkjet printed sensors.

The contents of this work are arranged as follows. Firstly, for preliminaries, inkjet-printing technology and ESN are introduced and explained in Section II. This section is followed by the sensor design and fabrication process in Section III. The sensor testing and data collection process is explained in Section IV, and data augmentation process is discussed in Section V. ESN model and its hyperparameters optimization is explained in Section VI. Lastly, the result is analysed in Section VII and followed by a conclusion in Section VIII.

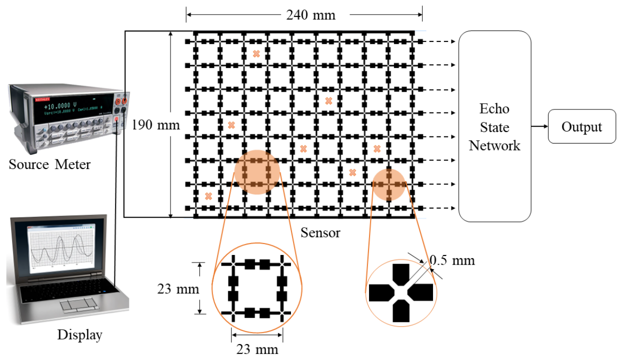

Fig. 1: Experimental setup for pencil drop experiment in the grid tactile sensor along with ESN. Grid tactile sensor is current biased with source Meter Unit (SMU). All relevant dimensions of the sensor is showed. Here, X-mark indicates the randomly chosen areas for pencil impact experiment in the tactile sensor grid. Dotted line from sensor to ESN indicates the optional connection.

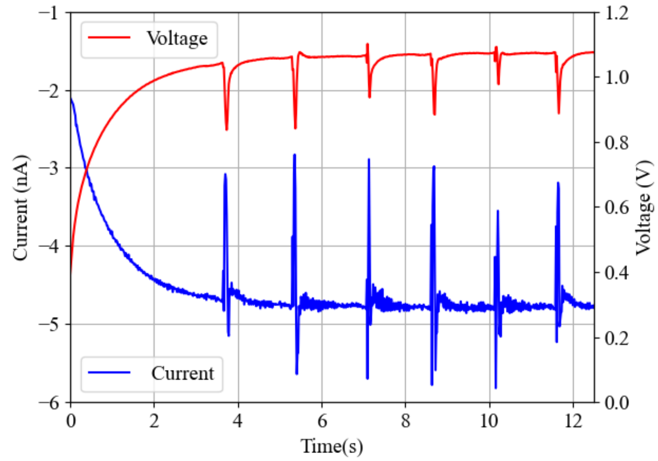

Fig. 2: Current and voltage signal for multiple pencil drops in a random point of tactile sensor grid. Each disturbance in the graph represents a pencil drop in the grid sensor.

II. Preliminaries

A. Echo State Network

Echo State Network is a type of recurrent neural network introduced by Jaeger in 2007 [13]. It has gained significant popularity within the field of RC. It contains three layers named a input layer, reservoir and output layer, which is also known as readout layer, solely trainable layer in the model. Dynamics and output update laws are defined by equations (1) and (2).

$$x(n+1) = f(W_{in}u(n+1) + W_{res}x(n)) \tag{1}$$

$$y(n+1) = W_o x(n+1) \tag{2}$$

where u(n) indicates the input vector fed into the ESN, x(n) is the reservoir state vector, and y(n) is the output state vector at time n. W_{in}, W_{res}, and W_o are the input, reservoir, and output layer weight matrix, respectively, and f(.) is the non-linear activation function. To achieve the echo state property of the reservoir weight, it needs to be scaled by spectral radius λ_{max}. In a sparsely connected reservoir, 5-10% weights are nonzero, and the readout layer is trained by a simple linear regression method [14] [15].

$$y = W_o \Phi + \epsilon \tag{3}$$

where,

$$\Phi = [x(n), x(n+1), \ldots, x(n+N-1)]^T$$
$$y = [y(n), y(n+1), \ldots, y(n+N-1)]^T$$

Here, n is the stating index of the training samples, which is initially set to discard the influence of reservoir initial transient. ϵ is assumed to be zero-mean Gaussian noise with β variance and N is the number of training samples.

As there is only one simple trainable layer, ESN is a low computation-intensive network. Therefore, ESN is broadly used in different areas, such as pattern recognition, time series data analysis, anomaly detection system modeling and control, etc.

III. Inkjet Printed Sensor Fabrication

In our research, an inkjet-printed tactile sensor array is developed which is capable of localizing impacts. This sensor is inkjet printed on a polyethylene terephthalate (PET) film substrate of 180 mm by 215 mm in size. A standard drop-on-demand piezoelectric printer is used to print with silver nanoparticles on PET film with a thickness of 135μm. After printing, the sensor was thermally cured on a hotplate for a specified duration. The grid is created by 8 horizontal lines with 240 mm along with 10 vertical lines with 190 mm. All of these lines are spaces by 23 mm and features a 0.5 mm gap at each intersection, which is acting as a capacitive sensing point and exhibiting nonlinear voltage-current characteristics. Fig. 1 depicts all relevant dimensions of the sensor array along with the experimental setup.

This inkjet-printed tactile sensor grid translates location impacts into a high-dimensional signal profile. For current biasing, two opposite sides of 10 vertical lines of the grid are interconnected, while the remaining 8 horizontal lines are configured for signal acquisition. From these 8 horizontal lines, any number of connection can be randomly selected for integration with an ESN. In this particular study, only one of these lines are chosen randomly to connect with the ESN for further analysis.

IV. Sensor Testing and Data Collection

After fabrication, the sensor's performance was tested via a pencil drop experiment. The sensor grid was tested using a Keithley 2604B Dual channel Source Meter Unit (SMU), applying a consistent current bias of 0.5 nA. In this evaluation,

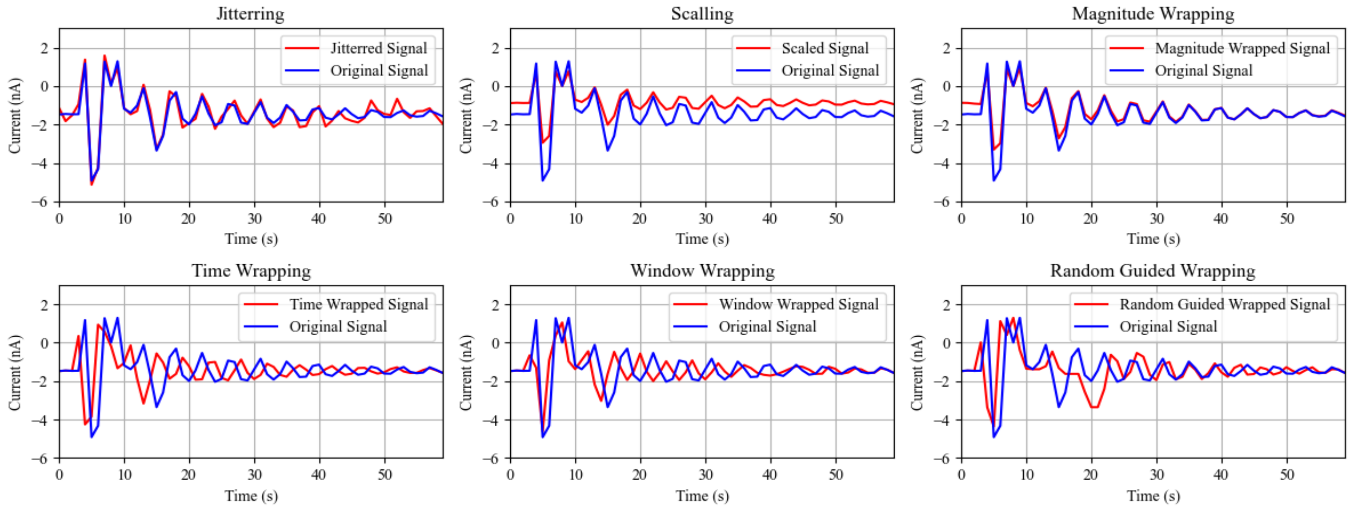

Fig. 3: Original current signal occurred from pencil drop and transformed current signal after data augmentation is showed in two different colors. For magnitude domain data augmentation method jittering, scaling and magnitude wrapping is applied as well as for time domain data augmentation time wrapping, widow wrapping and random guided wrapping is applied.

a pencil was repeatedly dropped from a set height onto 12 randomly selected points on the sensor grid. In the Fig. 1 those randomly selected points are showed with X-mark. For each impact, current signal was captured from one arbitrarily chosen line out of the available 8 horizontal lines to compile time series information. Fig. 2 illustrates the sensor's current and voltage fluctuations corresponding to each pencil impact in a randomly chosen area for pencil drop. After an impact, the sensor typically records around 60 sampling time before stabilizing and be prepared for next pencil drop. A method of window slicing was utilized to isolate individual pencil drop events within the current signals. Each randomly selected area in the grid was on average subjected to five pencil drops, resulting in a total of 61 time series signals. This dataset with 61 time series signals subsequently utilized for the training and testing of the machine learning algorithm with 7:3 ratio. For testing around 19 time series signals are used for testing and, 42 time series signals are used for training. However, before training data augmentation is used in these 42 time series signal to make the model more robust.

V. Data Augmentation

Data augmentation is a widely used technique in computer vision and has been shown to enhance generalization in neural networks when applied to time series data. It involves the random alteration of data in two key aspects: time and magnitude. Historically, the addition of noise and scaling have been effective for augmenting data in the magnitude domain of time series. In our research, we have adopted the jittering approach to introduce gaussian noise, $\mathcal{N}(\mu, \sigma^2)$ is added to each time steps of the time series signal. In the gaussian noise mean μ is set zero and standard deviation σ is tuned according to required signal to noise ratio. Additionally, we've

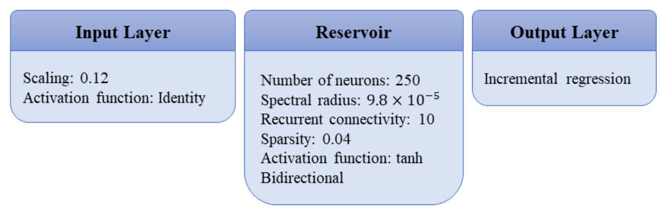

Fig. 4: ESN contains three layers: input layer, reservoir and output layer. Hyperparameters of these layers are showed.

implemented scaling and magnitude wrapping to modify the magnitude characteristics of time series data [16].

In our data augmentation process, we have incorporated five specific methods for enhancing robustness: time wrapping, window wrapping, sub-optimal wrapping, random guided wrapping, and discriminative guided wrapping, in addition to magnitude wrapping. Fig. 3 transformed time series signal is showed along with original current signal. These techniques contribute to building a stronger dataset that facilitates neural network training, enabling it to discern and learn from a diverse array of patterns and subtle variations. Our aim is for the model to develop a resilient and generalize understanding that can withstand fluctuations in either the magnitude or time aspects of the data. For instance, applying magnitude warping combined with Gaussian noise mimics various real-life disruptions, like those stemming from measurement inaccuracies or signal artifacts due to physical movements of the subject. The time-domain transformations are designed to reflect variations in the sensor's recovery time following events such as a pencil drop, further enhancing the model's ability to generalize from the sensor data. By applying data augmentation in training time series signals, 42 time series signals are increased into 588 time series signals which is used for training.

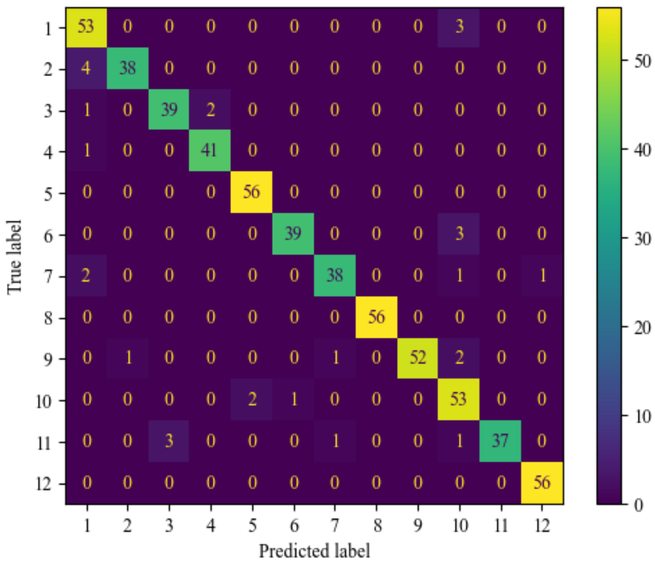

Fig. 5: Confusion matrix for ESN classification model. Matrix shows the desired output along Y axis and ESN model predicted output along X axis. Diagonal elements are showed the correctly predicted output, whereas non-diagonal elements are showing wrongly predicted output. Pencil drop areas are indicated as number and larger number indicates the areas closer to data collection line.

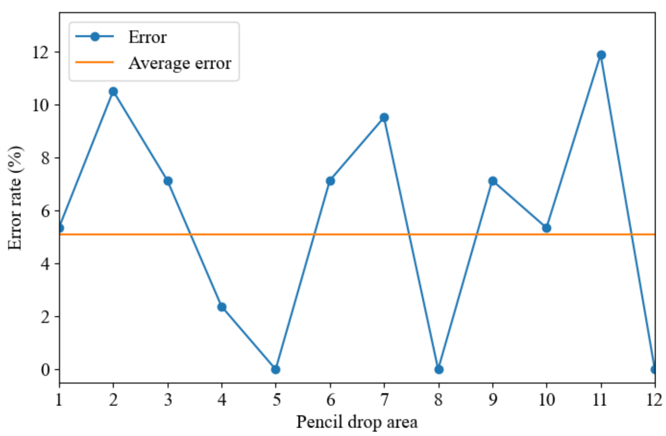

Fig. 6: Visualization of error rate of the different areas of pencil drop experiment along with average error rate.

VI. ESN Hyperparameters Optimization

This section details the ESN model development for the time series signal classification. ESN model is developed with learning rate and leakage of $1 \times 10-5$ and 1 respectively. In the input layer, reservoir and output layer, there are more hyperparameters which are determined by optimization process.

Optimization is the process of finding the optimal set of hyperparameters for a machine learning model that maximizes its performance on a given dataset. For hyperparameters optimization of a model there are some common methods such as random search, grid search etc. The choice of hyperparameter optimization technique depends on factors such as the complexity of the model, the size of the hyperparameter space, and the computational resources available. The goal is to find a good set of hyperparameters in a reasonable amount of time, improving the model's performance on the task at hand.

By using PyRCN interface, hyperparameters of ESN are optimised [17]. Initially model starts with some fixed parameters such as, hidden layer size, spectral radius, input scaling, leakage etc. For the optimization of input scaling, spectral radius and bias scaling sequential search is done in the uniform distribution of these parameters within a certain range. Moreover, for leakage and alpha sequential search is performed in logarithmic uniform distribution of these parameters. Other hyperparameters, including input and reservoir activation functions, decision strategy, and bidirectional connectivity, remain constant initially. The sequential search process identifies the best hyperparameters for the model, which are presented in Fig. 4. For reservoir activation function hyperbolic tangent function is used.

VII. Classification and Performance Results

Proposed ESN network with optimised hyper parameter is trained with original training dataset stacked with its augmented versions. Average training and validation accuracy for the proposed model is 94.89% and 94% respectively. In the Fig. 5 confusion matrix of the ESN model is showed. True labels are showed in Y axis and predicted labels are showed in X axis. Areas closer to the data collecting points are indicated by larger numbers. From confusion matrix it is evident that pencil drop points closer to the data collection point are more accurately classified whereas error rates are quite large for the distant areas from data collection areas. Fig. 6 shows the classification error rate of all points along with the average classification error rate. Propagation path and charge sharing of grid causes this periodic error rate relation with pencil drop areas. Effect of propagation path in impact localization is a matter of future objective. Without the use of data augmentation, there's a risk of overfitting, while the complexity of ESN models must be increased to enhance accuracy. Moreover, by tweaking the value of some hyperparameters like spectral radius, leakage accuracy can be increased, however it will throw the model towards overfitting.

VIII. Conclusion

This research developed a tactile grid sensor utilizing inkjet printing technology and silver nanoparticle ink. Printed onto PET film using a standard office printer, the sensor's simple crossbar grid design enables the capture of time series data from pencil impact tests, with impacts occurring at random grid locations. The collected data is processed by an ESN to classify the location of each impact. To train the ESN, the original time series signal is augmented with time and magnitude domain transformations, enhancing the model's resilience to real-world signal distortions, such as noise caused by sensor movement. The grid design converts the sensory input into a multidimensional signal. Hyperparameter optimization for the ESN is performed through sequential searches within uniform and log-uniform distributions, fine-tuning the network's performance. By integrating inkjet printed sensor technology with artificial intelligence, this study overcomes the typical efficiency constraints of conventional inkjet printed sensors. The resulting sensor is not only cost-effective and versatile but also suitable for an array of uses, including structural health monitoring in infrastructure, automobile industry and robotics. The sensor's adaptability is particularly beneficial for creating personalized wearable monitoring and damage tracking in automobile, with the flexibility to conform to non-uniform surfaces, such as the inside of a helmet or any protective gear, to measure impact force and exposure accurately.

ACKNOWLEDGMENT

We are grateful to Mohammad Muklasur Rahman Opu for his assistance with data collection and Dr. Steven D. Gardner for his insight and expertise. This work was supported by the USA National Science Foundation (NSF) under Grant no. ECCS-2201447. Any opinions, findings, and conclusions or recommendations expressed in this material are those of the author(s) and do not necessarily reflect the views of the National Science Foundation.

REFERENCES

[1] E. Pritchard, M. Mahfouz, B. Evans, S. Eliza and M. Haider, "Flexible capacitive sensors for high resolution pressure measurement," *SENSORS, 2008 IEEE*, Lecce, Italy, 2008, pp. 1484-1487.

[2] W. Qu, S. K. Islam, M. R. Mahfouz, M. R. Haider, G. To and S. Mostafa, "Microcantilever Array Pressure Measurement System for Biomedical Instrumentation," in *IEEE Sensors Journal*, vol. 10, no. 2, pp. 321-330, Feb. 2010, doi: 10.1109/JSEN.2009.2034134.

[3] M. R. Haider, S. K. Islam, S. Mostafa, M. Zhang and T. Oh, "Low-Power Low-Voltage Current Readout Circuit for Inductively Powered Implant System," in *IEEE Transactions on Biomedical Circuits and Systems*, vol. 4, no. 4, pp. 205-213, Aug. 2010.

[4] N. Kuboki, H. Okamura, T. Enomonto, T. Nishimoto, T. Ohue and K. Ohue. "An occupant sensing system for automobiles using a flexible tactile force sensor." *Furukawa Review* , vol. 20, pp. 89–94, 2001.

[5] L. Kogan, T. L. Weadon, T. Evans, D. B. DeVallance, and E. M. Sabolsky. "Testing of tactile sensors for space applications." *Sensors and Smart Structures Technologies for Civil, Mechanical, and Aerospace Systems* , vol. 9435, pp. 691–697, 2015.

[6] S. Wang, and S. Zhu. "Impact source localization and vibration intensity prediction on construction sites." *Measurement* , vol. 175, pp. 109148, 2021.

[7] M. R. Opu, S. D. Gardner and M. R. Haider, "A Low-Cost Inkjet-Printed Heart Sound Sensor for Telehealth Application," 2023 IEEE 66th International Midwest Symposium on Circuits and Systems (MWSCAS), Tempe, AZ, USA.

[8] R. Lu, A. K. M. Arifuzzman, M. K. Hossain, S. Gardner, S. A. Eliza, J. I. D. Alexander, Y. Massoud, and M. R. Haider, "A Low-Power Sensitive Integrated Sensor System for Thermal Flow Monitoring," *IEEE Transactions on Very Large Scale Integration (VLSI) Systems*, vol. 27, no. 12, pp. 2949–2953, Dec. 2019.

[9] S. Gardner, A. Porbanderwala and M. R. Haider, "An Affordable Inkjet-Printed Foot Sole Sensor and Machine Learning for Telehealth Devices," *IEEE Sensors Letters*, vol. 7, no. 6, pp. 1-4, June 2023.

[10] S. D. Gardner and M. R. Haider, "An Inkjet-Printed Artificial Neuron for Physical Reservoir Computing," *IEEE Journal on Flexible Electronics*, vol. 1, no. 3, pp. 185–193, July 2022.

[11] S. D. Gardner, M. R. Opu and M. R. Haider, "An Inkjet-Printed Capacitive Sensor for Ultra-Low-Power Proximity and Vibration Detection," 2023 IEEE Wireless and Microwave Technology Conference (WAMICON), Melbourne, FL, USA, 2023.

[12] S. D. Gardner, J. I. D. Alexander, Y. Massoud and M. R. Haider, "Minimally produced inkjet-printed tactile sensor model for improved data reliability," 2020 11th International Conference on Electrical and Computer Engineering (ICECE), Dhaka, Bangladesh.

[13] H. Jaeger, "The 'echo state' approach to analysing and training recurrent neural networks-with an erratum note," German Nat. Res. Center Inf. Technol., Karlsruhe, Germany, GMD Tech. Rep. 148, 2001.

[14] H. Jaeger, "Tutorial on training recurrent neural networks, covering BPTT, RTRL, EKF and echo state network approach," German National Research Center for Information Technology, St. Augustin, Germany, Tech. Rep. 159, 2002.

[15] H. Jaeger, "Advances in neural information processing systems," *Advances in Neural Information Processing Systems*. Cambridge, MA: MIT Press, 2003.

[16] B. K. Iwana and S. Uchida, "An empirical survey of data augmentation for time series classification with neural networks," *PLoS ONE*, vol. 16, no. 7, Jul. 2021.

[17] P. Steiner, A. Jalalvand, S. Stone, and P. Birkholz, "PyRCN: A toolbox for exploration and application of Reservoir Computing Networks," *Engineering Applications of Artificial Intelligence*, vol. 113, p. 104964, 2022.